# Effect of Monomer Geometry on the Fractal Structure of Colloidal Rod Aggregates

Ali Mohraz, David B. Moler, Robert M. Ziff, and Michael J. Solomon
*University of Michigan, Ann Arbor, Michigan 48109, USA*
(Received 26 September 2003; published 14 April 2004)

The fractal structure of clusters formed by diffusion-limited aggregation of rodlike particles is characterized over three decades of the scattering vector $q$, and displays an unexpected dependence on the aspect ratio of the constituent monomers. Monte Carlo simulations of aggregating Brownian rods corroborate the experimental finding that the measured fractal dimension is an increasing function of the monomer aspect ratio. Moreover, increasing the rod aspect ratio eliminates the structural distinction between diffusion- and reaction-limited cluster aggregation that is observed for spheres.

DOI: 10.1103/PhysRevLett.92.155503 PACS numbers: 61.43.Hv, 82.70.Dd

Colloidal aggregation and gelation are principal examples of disordered growth under conditions far from equilibrium. A quantitative characterization of these phenomena is valuable to understanding complex shapes and forms that naturally assemble through nonequilibrium pattern-formation processes. These processes have thus long been subject to intense scientific study; basic principles of colloidal aggregation are reviewed in Refs. [1,2]. Moreover, the disordered structures that arise due to the nonequilibrium aggregation of multiple colloids exhibit scale-invariant properties described by fractal geometry [3–7]. Aggregation kinetics display two limiting regimes [8]. In the first, particles form rigid bonds upon collision, resulting in the fast aggregation kinetics of diffusion-limited cluster aggregation (DLCA). In the second, slower process, called reaction-limited cluster aggregation (RLCA), only collisions that overcome an energy barrier result in irreversible particle-particle bonds. Early research focused on the aggregation of spherical particles as a model system. These studies showed that colloidal aggregation displays universal characteristics including, in particular, fixed values of the cluster fractal dimension in the DLCA and RLCA regimes [9]. The claim of universality stems from studies in which colloidal chemistry and interparticle interactions were varied [10,11]. More recently, additional universal properties of aggregating spherical colloids have been reported [12–15].

In this Letter we extend the range of possible structures resulting from nonequilibrium aggregation by generating clusters composed of rod-shaped colloidal monomers. We find a family of fractal objects with structure that can be tailored by manipulation of the colloidal rod aspect ratio. The structures formed are characterized by light scattering, and the underlying physics of the aggregation process is probed by Monte Carlo simulation of the rod clusters. Our findings identify a set of previously unknown DLCA structures that arise due to the interaction of Brownian motion and anisotropic excluded volume. The effect of this interaction on cluster structure surprisingly persists to scales that are at least many hundreds of times greater that the monomer major axis. We explain the results in light of the geometric role of the anisotropic excluded volume of the primary rod monomers in mediating the scaling between the mass of a cluster aggregate and its characteristic size. While the role of monomer shape anisotropy in the formation of equilibrium liquid crystal phases has long been known [16], this report describes unforeseen implications of this parameter for amorphous, isotropic structures that facilitate a better understanding of the unusual rheology [17], sedimentation [18], packing [19], percolation [20], and self-assembly of anisometric colloids [21] and nanorods [22].

Colloidal boehmite (AlOOH) rods with approximately monodisperse dimensions were synthesized [23]. The mean major and minor axes and aspect ratio of the particles, denoted by $a$, $b$, and $r = a/b$, respectively, were characterized by analysis of at least 50 particles imaged by transmission electron microscopy. Particles with aspect ratios of $r_1 = 3.9$ ($a_1 = 52.2 \pm 16$ nm, $b_1 = 13.5 \pm 3.5$ nm), $r_2 = 8.6$ ($a_2 = 101.7 \pm 25$ nm, $b_2 = 11.8 \pm 3.4$ nm), and $r_3 = 30.1$ ($a_3 = 253.1 \pm 30.4$ nm, $b_3 = 8.41 \pm 1.3$ nm) were studied. Aggregation in stable aqueous suspensions was induced with either $MgCl_2$, $Na_2SO_4$, or NaOH.

The terminal internal structure of the clusters was quantified over a range of three decades of the scattering vector, $q$, by combined ultrasmall, small, and wide-angle light scattering (USALS, SALS, and WALS). The USALS apparatus ($\lambda_0 = 0.633$ $\mu$m) [24] probed the range of scattering vectors $0.0461\ \mu\text{m}^{-1} < q < 1.85\ \mu\text{m}^{-1}$. The SALS range ($\lambda_0 = 0.532$ $\mu$m) [25] was $0.822\ \mu\text{m}^{-1} < q < 6.76\ \mu\text{m}^{-1}$. WALS ($\lambda_0 = 0.488\ \mu$m) was performed on an ALV compact goniometer system (Langen, Germany) with $3.58\ \mu\text{m}^{-1} < q < 33.1\ \mu\text{m}^{-1}$. Measurements were conducted 3 h after initiation of the aggregation process, at colloid volume fraction $\phi = 10^{-4}$. Kinetic studies ascertained that this duration was sufficient to achieve a fully developed structure over the entire detectable range of the scattering vector for all aspect ratios studied.

To extract the structure factor, $S(q)$, intensity measurements were divided by the form factor of an ensemble of

  

randomly oriented rods in the Rayleigh-Gans-Debye approximation as warranted by previous calculations for arbitrarily shaped particles [26]. Figure 1 plots $S(q)$ of clusters composed of rods of the three different aspect ratios for the DLCA regime versus the dimensionless product of the scattering vector, $q$, and the particle major axis half-length, $a/2$. $S(q)$ for DLCA-aggregated polystyrene spheres ($a = 24$ nm) in a density-matching mixture is also plotted. While transient structure factor measurements exhibited curvature at low $q$ that is characteristic of finite aggregate size [12], these effects progressively shifted to smaller $q$ with time and were not observed at steady state. To assess reproducibility, one data set ($r = 8.6$) plots the average of nine independent experiments. For these measurements, the average standard deviation is 11%. The power-law scaling of $S(q)$ over an extensive range of $q$ indicates the clusters possess a self-similar structure. Also apparent in clusters composed of high-$r$ rods is a gradual crossover to nonfractal behavior at the highest $q$. Independent of aspect ratio, we find that this transition occurs at $qa/2 \sim 1$. The measured fractal dimension, $D_f$, of each aggregated sample, extracted by a power-law fit to the data for $qa/2 < 0.3$, is reported in the Fig. 1. The standard deviation in $D_f$ from the nine independent experiments for $r = 8.6$ is 3%.

To evaluate physicochemical conditions for the DLCA regime, the aggregation kinetics were examined by measuring the intensity autocorrelation function (ALV-5000E digital correlator, Langen, Germany) at $q = 24.2\ \mu\text{m}^{-1}$ during aggregation. The first cumulant, $\Gamma_1$, was determined from the initial decay rate ($t < 8$ ms) of the electric field autocorrelation function $g_1(t)$, where $\Gamma_1^{-1}$ is proportional to a measure of the effective cluster hydrodynamic radius. The evolution of $\Gamma_1^{-1}$ for the aggregation of colloidal rods with aspect ratio $r = 3.9$ at volume fraction $\phi = 1.5 \times 10^{-5}$ for various electrolytes is shown in the inset of Fig. 1. The concentrations $[\text{MgCl}_2] <$ 50 mM resulted in RLCA behavior as evidenced by the significant retardation of the aggregation kinetics. Addition of $Na_2SO_4$ or NaOH resulted in saturated DLCA kinetics above a particular electrolyte concentration. Comparable results were obtained for tests at higher $\phi$ and different $r$.

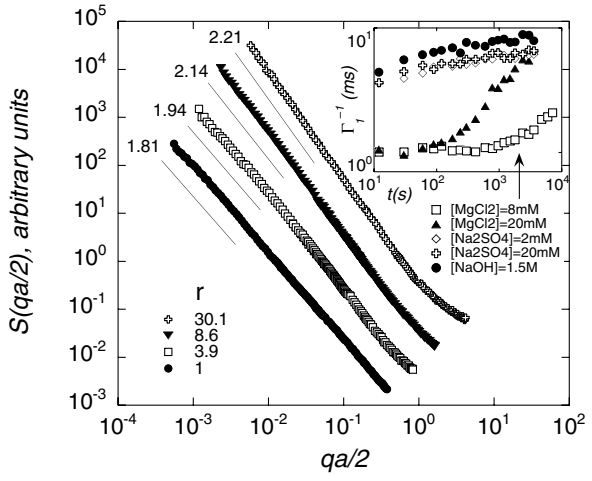


FIG. 1. Structure factor of DLCA clusters for various monomer aspect ratios ($r = 1$ corresponds to spheres). Data are offset for clarity. Drawn lines correspond to the measured fractal dimensions. The inset plots the aggregation kinetics at various electrolyte concentrations.

Figure 1 reports the remarkable result that the $D_f$ of DLCA clusters is an increasing function of the monomer aspect ratio. This result is unexpected in light of the universal behavior of DLCA colloidal sphere aggregation [11]. The difference between the DLCA fractal dimension of clusters composed of spheres ($D_f = 1.81 \pm 0.02$) and of rods with $r = 30.1$ ($D_f = 2.26 \pm 0.18$) is much greater than the uncertainty in its characterization, and is as significant as the difference between the DLCA and RLCA fractal dimensions in spheres. Figure 1 demonstrates that clusters with radius $> 10^2 a$ are still strongly influenced by the geometry of the monomer. This persistent effect of primary particle geometry on the structure of nonequilibrium aggregates indicates that the anisotropic excluded volume of the colloidal rods affects the cluster-cluster aggregation mechanism in an unforeseen manner.

Monte Carlo simulations were used to independently probe the dependence of $D_f$ on the monomer aspect ratio. We developed a minimal model of Brownian rod DLCA by adapting the early methods for DLCA of spheres [5,6,27]. Simulations were carried out off-lattice in a periodic $L \times L \times L$ space, initially populated with $N$ randomly oriented rods, each constructed by linearly aligning $r$ spheres [28]. For each Monte Carlo step, $t$, a cluster (or primary rod) was chosen at random and moved with probability equal to its mobility, $\mu_{i,t} = Rg_{\min,t}/Rg_{i,t}$, where $Rg_{i,t}$ and $Rg_{\min,t}$ are the radii of gyration at step $t$, of the cluster $i$ and the smallest cluster present, respectively [29]. Aggregates composed of two or more rods were moved in a random direction while primary rods were moved according to the translational diffusion of a prolate spheroid of aspect ratio $r$ [30]. Clusters were moved a distance equal to $a/2$ if there were no obstacles in their path. In the event that a full move would result in a collision, the clusters were merged at the point of intersection. This process was continued until the first cluster with $Rg = L/4$ was detected. This model of colloidal rod DLCA neglects some interesting physics such as the rotational diffusion, hydrodynamic interaction, and internal rearrangement of clusters due to Brownian forces. However, even this minimal model, comparable in complexity to the classical work of Meakin on spherical particles [27], is sufficient to establish the role of monomer aspect ratio in the structure of DLCA aggregates.

Figure 2 is a logarithmic plot of $Rg$ vs mass of the cluster for various particle aspect ratios from the simulations. The fractal dimension, $D_f$, is the inverse of the slope obtained from a linear fit to the data in the range of

cluster masses, $M$: $[4M_{\min}, M_{\max}]$, where $M_{\min}$ and $M_{\max}$ are the masses of an individual rod and the largest cluster present in the simulation, respectively. Parametric sensitivity of the model was tested by varying $\phi$, step size, and by incorporating isotropic translational diffusion for primary rod particles. $D_f$ showed a slow increase with $\phi$, but was insensitive to the other changes. We therefore performed simulations at a low, fixed $\phi = 1.3 \times 10^{-3}$. Figure 2 shows that the simulated DLCA of rods yields clusters with measured fractal dimension that increases with monomer aspect ratio, just as observed for the experiments. The Fig. 2 inset compares 2D projections of terminal structures for particles with $r = 11$ and $r = 1$. The more highly branched $r = 11$ cluster results in a larger measured fractal dimension.

Mean values of $D_f$ obtained from experiments and simulations are compared in Fig. 3. Standard deviations were generated by repeating the experiments at least 5 times and by performing the simulations with at least five different initial seeding conditions (three seedings were used for $r \geq 9$). Good agreement between the experiments and simulations is obtained. The finding establishes, by two different methods, the profound effect of monomer geometry on the measured fractal dimension of clusters that evolve as colloidal particles undergo diffusion-limited cluster aggregation.

Possible origins of the small difference between $D_f$ of the experiments and simulations are the dimensional polydispersity of the primary particles used in the experiments and any local annealing of the rods to the more energetically favored parallel orientation after the initial aggregation event. Although the probability of such internal rearrangements could itself depend on the aspect ratio of the monomers, Fig. 3 indicates that this effect is likely small. To investigate possible effects of the sedimentation of dense rods ($\Delta\rho/\rho \sim 2$) USALS measurements were executed both immediately after the structure had developed, and after sedimentation of aggregates to less than half the total sample volume had occurred ~40 h later. No distinguishable difference was observed in the measured fractal dimension. Therefore, the observed marginal discrepancy is not likely an effect of sedimentation. However, the precise role of a finite sedimentation velocity on Brownian rod aggregation is a complex question that warrants future investigation.

In Fig. 4 we plot $S(q)$ of aggregated colloidal rods with $r = 3.9$ and $r = 30.1$ for both regimes and report that rod aggregation leads, as $r$ is increased, to a loss of distinction between the DLCA and RLCA terminal structures. Measured values of $D_f$ are reported for various values of $r$ in the figure inset, together with those for polystyrene spheres ($a = 24$ nm) in a density-matching solvent (data not shown for clarity). The difference between the fractal dimensions of the two regimes diminishes as the degree of anisotropy in the monomer geometry increases. For spheres, the distinction between structures in the two regimes stems from the enhanced possibility of particles and small clusters to diffuse into the larger tenuous aggregates in the RLCA process. Because the DLCA and RLCA fractal dimensions are similar, this densification mechanism is apparently excluded at high $r$. Likely, rods and small rod aggregates have smaller probability relative to spheres of penetrating the growing RLCA clusters because the effective excluded volume per unit mass carved out by the rotational diffusion of a rod is greater than that of spheres by the large factor $r^2$. In addition, DLCA clusters of high aspect ratio rods are already denser relative to those of spheres, as indicated by their larger values of $D_f$. Thus, for rods, most paths into the cluster interior are blocked and the slower RLCA process yields little incremental densification relative to DLCA.

In conclusion, we discuss the mechanism responsible for the observed deviation of rod aggregation from the universal behavior found for colloidal spheres by the following two-body geometric argument: Consider the aggregation of a spherical particle with another. Let $l$ be the distance between the particle centers of mass at

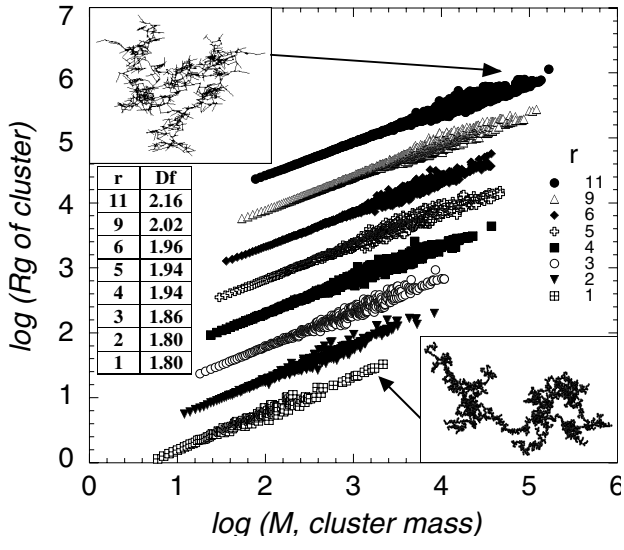


FIG. 2. Scaling of $Rg$ with cluster mass, from Monte Carlo simulations. Data are offset for clarity. The inset compares the terminal structure of $r = 11$ and $r = 1$ (sphere) aggregates.

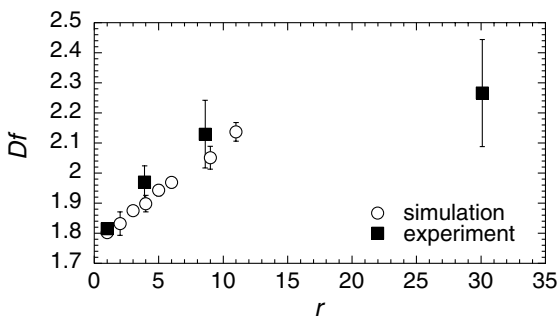


FIG. 3. Comparison of the measured fractal dimension versus particle aspect ratio from experiments and simulations.

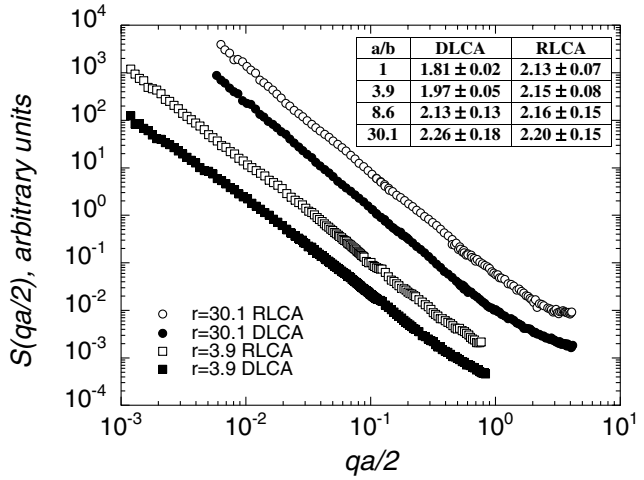


| a/b | DLCA | RLCA |
|---|---|---|
| 1 | 1.81 ± 0.02 | 2.13 ± 0.07 |
| 3.9 | 1.97 ± 0.05 | 2.15 ± 0.08 |
| 8.6 | 2.13 ± 0.13 | 2.16 ± 0.15 |
| 30.1 | 2.26 ± 0.18 | 2.20 ± 0.15 |

FIG. 4. Structure factor of colloidal rods in the DLCA and RLCA regimes for $r = 3.9$, and $r = 30.1$. $D_f$ is reported for various values of $r$ in the inset table.

aggregation. For spheres, $l = a$ ($a$ = particle diameter) uniquely, and thus $l/2 >$ Rg of an individual sphere since $Rg$, sphere $= a/\sqrt{10}$. In contrast, the anisotropy of excluded volume for cylindrical rods yields $Rg$ for rotation about the major axis, $Rg$, major $= (b^2/16 + a^2/12)^{1/2}$ and, for rotation about the minor axis, $Rg$, minor $= b/\sqrt{8}$. Thus, a portion of the possible contacts of a test rod particle with another will occur such that $l/2 < Rg$, major. On a per unit mass basis, these contacts act to decrease the mean cluster $Rg$ relative to that of spheres, thereby resulting in a tendency toward denser clusters and a larger measured fractal dimension.

Clearly, this qualitative explanation, based on a two-body interaction, is a simplification of the resulting many-body structure. However, additional analysis of the Monte Carlo simulations (data not shown) indicate that such two-body interactions are sufficient to generate cluster structures that are monomer-aspect-ratio dependent. Moreover, the mechanism also allows the experiments and simulations to be reconciled with the perception that, for $q$ sufficiently small, scale invariance requires that structures resulting from cluster-cluster aggregation be independent of the details of monomer shape. As clusters grow, the probability of anisotropic excluded volume interactions decreases because the high aspect ratio monomers are increasingly incorporated into the less anisotropic clusters. Thus, as $q$ decreases the effect of rod shape on cluster structure should be increasingly damped. Yet, Fig. 1 demonstrates that clusters with sizes of order $10^2a$ still strongly display the effect of this anisotropic interaction. Apparently, the crossover to the asymptotic, universal DLCA behavior is unexpectedly slow and thus the initial effect of the primary monomer anisotropy on cluster structure is extraordinarily persistent.

Support for this study was provided by the NASA Fluid Physics Program (NAG3-2356). We acknowledge the participation of Mark Elsesser and Amy Herzog in this study.

[1] P. Meakin, *Fractals, Scaling and Growth Far from Equilibrium* (Cambridge University Press, Cambridge, 1998).
[2] W. B. Russell, D. A. Saville, and W. R. Schowalter, *Colloidal Dispersions* (Cambridge University Press, Cambridge, 1989).
[3] B. B. Mandelbrot, *The Fractal Geometry of Nature* (W. H. Freeman, New York, 1983).
[4] T. A. Witten and L. M. Sander, Phys. Rev. Lett. **47**, 1400 (1981).
[5] P. Meakin, Phys. Rev. Lett. **51**, 1119 (1983).
[6] M. Kolb, R. Botet, and R. Jullien, Phys. Rev. Lett. **51**, 1123 (1983).
[7] D. A. Weitz and M. Oliveria, Phys. Rev. Lett. **52**, 1433 (1984).
[8] *Kinetics of Aggregation and Gelation*, edited by F. Family and D. P. Landau (Elsevier, Amsterdam, 1984).
[9] D. A. Weitz, J. S. Huang, M. Y. Lin, and J. Sung, Phys. Rev. Lett. **54**, 1416 (1985).
[10] M. Y. Lin *et al.*, Phys. Rev. A **41**, 2005 (1990).
[11] M. Y. Lin *et al.*, J. Phys. Condens. Matter **2**, 3093 (1990).
[12] M. Carpineti and M. Giglio, Phys. Rev. Lett. **68**, 3327 (1992).
[13] M. Carpineti and M. Giglio, Phys. Rev. Lett. **70**, 3828 (1993).
[14] L. Cipelletti, S. Manley, R. C. Ball, and D. A. Weitz, Phys. Rev. Lett. **84**, 2275 (2000).
[15] D. Fry, T. Sintes, A. Chakrabarti, and C. M. Sorensen, Phys. Rev. Lett. **89**, 148301 (2002).
[16] P. G. de Gennes, *The Physics of Liquid Crystals* (Clarendon Press, Oxford, 1974).
[17] M. J. Solomon and D. V. Boger, J. Rheol. **42**, 929 (1998).
[18] A. P. Philipse, A. Nechifor, and C. Patmamanoharan, Langmuir **10**, 4451 (1994).
[19] A. P. Philipse, Langmuir **12**, 1127 (1996).
[20] E. J. Garboczi, K. A. Snyder, J. F. Douglas, and M. F. Thorpe, Phys. Rev. E **52**, 819 (1995).
[21] J. Parkinson, K. E. Kadler, and A. Brass, Phys. Rev. E **50**, 2963 (1994).
[22] W. U. Huynh, J. J. Dittmer, and A. P. Aliviastos, Science **295**, 2425 (2002).
[23] P. A. Buining, C. Pathmamanoharan, J. B. H. Jansen, and H. N. W. Lekkerkerker, J. Am. Ceram. Soc. **74**, 1303 (1991).
[24] F. Ferri, Rev. Sci. Instrum. **68**, 2265 (1997).
[25] P. Varadan and M. J. Solomon, Langmuir **17**, 2918 (2001).
[26] J. Buitenhuis, J. K. G. Dhont, and H. N. K. Lekkerkerker, J. Colloid Interface Sci. **162**, 19 (1994).
[27] P. Meakin, J. Colloid Interface Sci. **102**, 491 (1984).
[28] I. L. Claeys and J. F. Brady, J. Fluid Mech. **251**, 443 (1993).
[29] R. M. Ziff, E. D. McGrady, and P. Meakin, J. Chem. Phys. **82**, 5269 (1985).
[30] H. Brenner, Intern. J. Multiphase Flow **1**, 195 (1974).